Chapter 4

Fabrication of Coaxial Double-Shelled SiO_2/C Nanotubes

Abstract

The fabrication of Si/C-based composite nanostructures within the pores of anodic aluminum oxide is described. Employing the Na@AAO reactive template method, we synthesized coaxial doubled-shelled SiO_2/C nanotubules via multistage reactions involving hexachlorobenzene (C_6Cl_6), chlorosilanes and the Na incorporated template. We have carried out transmission electron microscopic (TEM) studies and electron energy loss spectroscopy (EELS) elemental mappings. From the EELS near edge structure of the C and Si K-edges, we conclude that the carbon is amorphous and the silicon is bounded to the oxygen neighbors. From the elemental mapping, we noted the Si layer is uniformly distributed inside the carbon layer.

4.1 Introduction

Since the first observation by Iijima,[1] there have been many reports[2-5] on the fabrication of CNT and related structures. This includes methods of producing nanostructures of uniform and well-aligned tubular arrays. An approach is based on template-assisted growth, by which carbon atoms are directly deposited in the pores of self-organized channels of anodic aluminum oxide (AAO) membranes from hydrocarbons by chemical vapor deposition (CVD) and related technologies.[6-9] Through this route, the size and shape of the nanotubes can be manipulated by the structure of the AAO templates effectively. After the template is removed, a free-standing array of aligned nanotubes can be obtained. Another important direction for template-based synthesis of micro- and nanostructures is the synthesis of composite multilayered materials. The experimental verification of the existence and the electronic

properties of such heteronanotubes is a topic of current research.[10-16]

In chapter 2, we reported an effective method to incorporate metallic sodium into the channels of AAO. The Na filled AAO (Na@AAO) can be employed as a "reactive template" to convert chlorocarbons via a stoichiometric Wurtz type C-C coupling reaction into well-aligned amorphous CNT (*a*-CNT) arrays.[17] In this chapter, we extend the method to fabricate multilayered materials. First, a layer of aligned *a*-CNT is deposited inside AAO substrate. Then, Na is incorporated into the composite template *a*-C/AAO. The template is reacted with a source of Si to grow multi-shelled coaxial nanotubes.

4.2 Experimental Section

The composite double-shelled SiO_2/C nanotubes were synthesized in a flow-tube furnace by using the Na@AAO method described in chapter 2.[17] The Na filled AAO can be employed as a "reactive template" to convert C_6Cl_6 via a stoichiometric Wurtz type C-C coupling reaction into well-aligned *a*-CNT arrays. Then, by decomposing NaH (Aldrich, 0.15 – 0.25 g, 6.3 – 10.4 mmol) with the as-formed *a*-C/AAO inside a tube furnace at 623 K under 1 atm of Ar (flow rate: 20 sccm) for 1 h, Na filled the channels of *a*-C/AAO to generate Na@*a*-C/AAO. Further reaction of Na@*a*-C/AAO with $SiCl_4$ and Si_2Cl_6 (Aldrich, vaporized at 273 K and 298 K, respectively) at 623 K for 6 – 21 h produced grayish black products. The products were immersed in 6 M HCl at 343 K for 6 h to remove the AAO membrane. Then, it was washed with boiling D.I. water and dried at 373 K in air to offer double-shelled SiO_2/C coaxial nanotubes. Microscopic features of the samples were observed with a scanning electron microscope (SEM, JEOL JSM-6330F at 15 kV) and a high resolution transmission electron microscope (HRTEM, Philips TECNAI 20 at 200 kV). Composition of the products was determined by energy dispersive spectroscopy (EDS, OXFORD Link Pentafet) and a parallel detection of electron energy loss spectroscopy (EELS, Gatan GIF 2001) in diffraction mode with a semi-collection angle approximately ~ 3.9 mrad. The K-edge of EELS of carbon,

oxygen and silicon were used for the energy filtered elemental mapping.

4.3 Results and Discussion

Figure 4.1 shows electron micrographs of vertically aligned double-shelled SiO_2/C nanotubes grown in AAO membranes from $SiCl_4$ and Si_2Cl_6 at 623 K by the sodium reactive template method. Figure 4.1 (a) shows an SEM image of the side view of a 60 μm SiO_2/C nanotubes bundle after the AAO removal. Figure 4.1 (b) shows one typical TEM image of the as prepared tubular product. In the open-end of the nanotube, along the direction normal to the "tube" axis, a layered structure with different phase composition along the vertical direction is observed. The product is not a simple "nanotube", but a wrapped composite nanotube, so-called "coaxial nanotube", which consists of an inner and an outer shell. The diameters of the inner shell and outer shell are approximately 268 nm and 290 nm with wall thicknesses as of 10 nm and 13 nm, respectively. Similar structures with the inner and outer nanotube diameters 260 nm and 300 nm and wall thicknesses 22 nm and 20 nm are seen in Figure 4.1 (c) and (d). This material was fabricated from Si_2Cl_6 with Na@*a*-C/AAO at 623 K. Typical electron diffraction (ED) patterns of individual tubes are shown in the insets in Figures 4.1 (b) and d. They are typical of amorphous materials. Energy dispersive X-ray spectra of the samples show signals only from carbon, oxygen, and silicon element. We also observed that there were gaps 5 - 24 nm in the interface of the coaxial nanotubes.

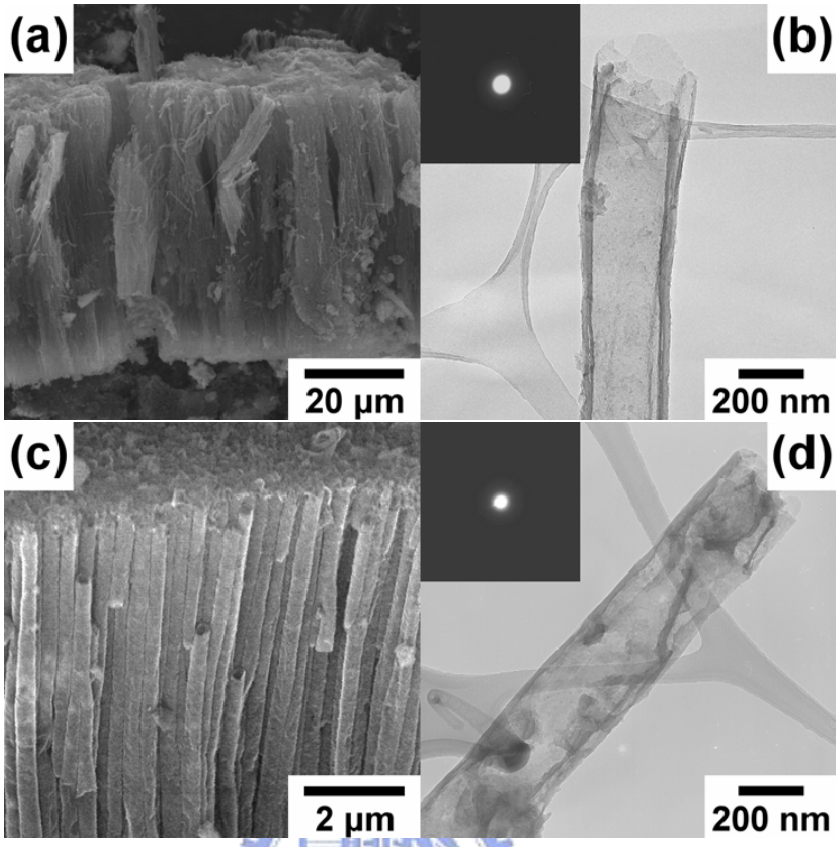

Figure 4.1 (a) SEM of a bundle of SiO_2/C nanotubes, and (b) TEM and ED of an isolated SiO_2/C nanotubes grown from $SiCl_4$ in Na@AAO at 623 K. The AAO was removed. (c) SEM of SiO_2/C nanotubes, and (d) TEM and ED of an isolated SiO_2/C nanotubes deposited from Si_2Cl_6 in Na@AAO at 623 K. The AAO was removed.

EELS characterization of the ionization K-edge for carbon, oxygen, and silicon was used to estimate the compositions and the chemical bounding state of the double-shelled nanotubes. The spectra were obtained using 5 - 10 nm probes. Typical EELS spectra from an individual nanotube are shown in Figure 4.2. Three distinct ionization edges at 284.0, 533.3, and 1841.4 eV corresponding to the characteristic K-shell ionization edges of C, O and Si K-edges, respectively. For the SiO_2/C nanotubes, the near edge finite structure of carbon K-edge in Figure 4.2 (a) consist of π* (284.0 eV) and σ* (295.4 eV) graphitic features.[18,19] The π* weak shoulder and distinct σ* antibonding orbitals, are the well-known signatures of the sp^3 type

bonding state of carbon atom where σ* region is the main feature. The overall signal shape is consistent with the known one of amorphous carbon.[20] In addition, there has a single broad peak of O K-edge at 533.3 eV in Figure 4.2 (a). The energy loss near edge structure (ELNES) reflects the site- and symmetry-projected density of states, and therefore it yields information on the electronic structure and on the oxidation state of the element under investigation.[21] The Si K-edge of a double-shelled nanotube is displayed in Figure 4.2 (b). The peak (1841.4 eV) in the Si K-edge spectrum can be attributed to the transition of Si 1s electron to the t_2* orbital with a majority of Si 3p character.[22,23] It can be seen that the primary Si K-edge peak of an amorphous SiO_2/C nanotubes corresponds to tetrahedrally coordinated Si. We have demonstrated above that the Si K-edge ELNES spectra provide a clear fingerprint of Si in a tetrahedral coordination environment. The O K-edge spectra also suggest that the Si and O are closely connected.[24,25]

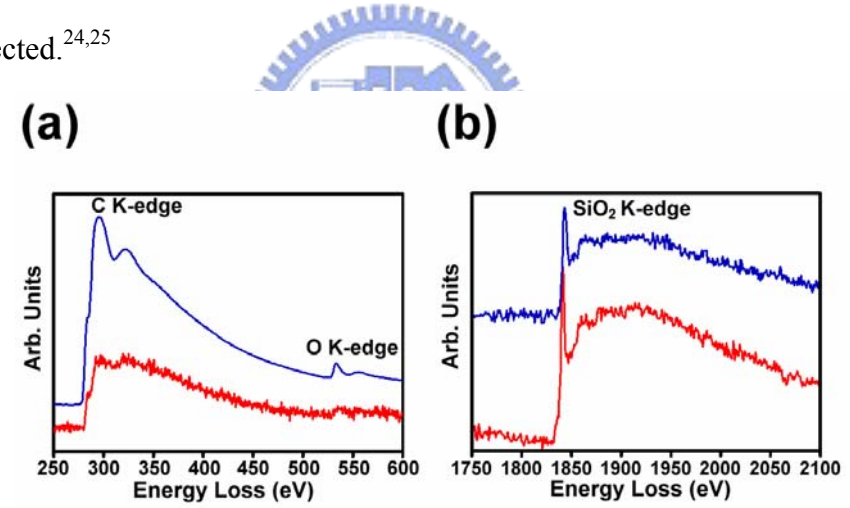

Figure 4.2 Representative EELS shown the existence of (a) C K-edge (284.0 eV), O K-edge (533.3 eV) and (b) Si K-edge (1841.4 eV) within the aligned double-shelled SiO_2/C nanotubes generated by reacting $SiCl_4$ (lower curve) and Si_2Cl_6 (upper curve) with Na@AAO at 623 K.

Figure 4.3 displays the EELS mapping images of double-shelled SiO_2/C nanotubes using the energy loss of K-shell edges. The outer diameters of the tubes are 290 nm and 280 nm, as shown in the zero loss images in Figures 4.3 (a) and 4.3 (d), respectively. Because a collection

of brighter point represents a higher concentration of the element, the observed distribution of the element is not uniform. Both C and Si maps show a pair of long straight bright contrast strips along the tube axis. The C map in Figure 4.3 (b) is consistent with a tube diameter of 290 nm and a wall thickness of 21 nm. We also obtained two straight dark lines inside the carbon layer. This area overlaps with the Si distribution map in Figure 4.3 (c). This suggests that a silicon shell with a diameter of 246 nm and a thickness of 18 nm resides insides the C shell. Figure 4.3 (d) - (f) show the images of the tube fabricated from Si_2Cl_6. The results are similar. The external carbon layer has a diameter of 280 nm and a wall thickness of 14 nm (Figure 4.3 (e)) while the internal silicon shell has a diameter of 220 nm and a wall thickness of 12 nm (Figure 4.3 (f)).

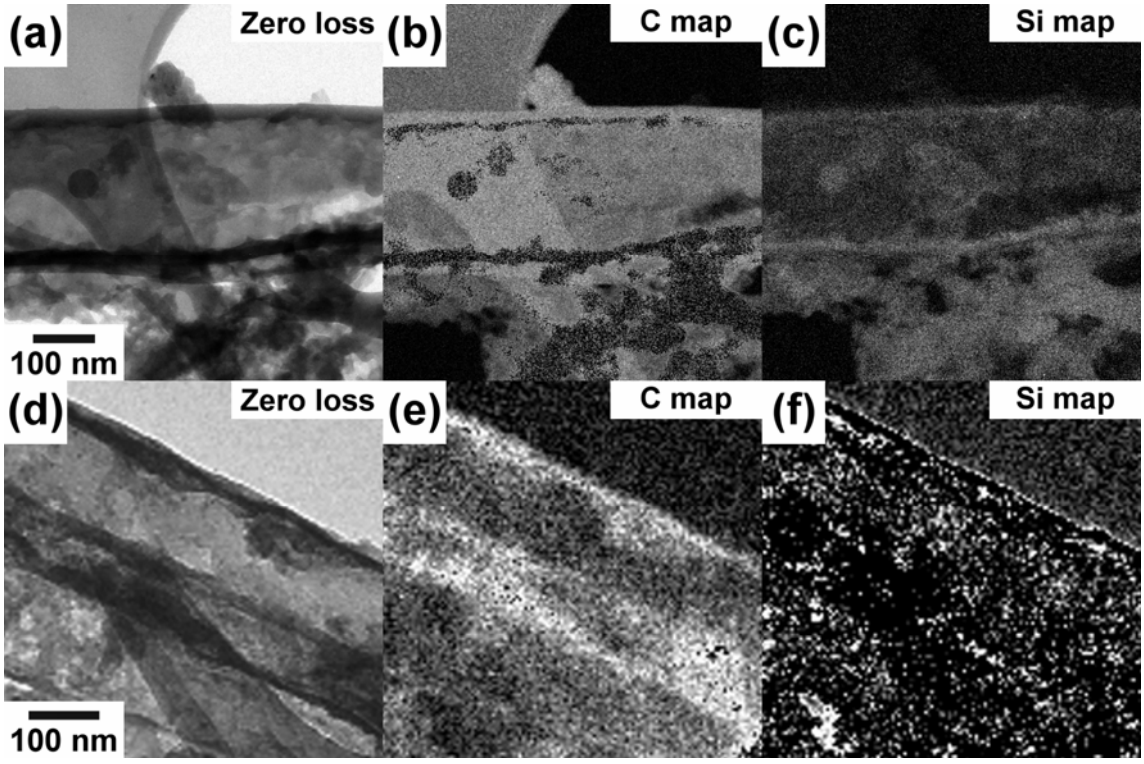

Figure 4.3 (a) TEM zero-loss image of an isolated SiO_2/C nanotubes grown from $SiCl_4$ at 623 K, (b) elemental C mapping of the image shown in (a), and (c) elemental Si mapping of the image shown in (a); (d) TEM zero-loss image of aligned double-shelled SiO_2/C nanotubes obtained from Si_2Cl_6 at 623 K, (e) elemental C mapping of the image shown in (d), and (f) elemental Si mapping of the image shown in (d).

Figure 4.4 shows the TEM image of an isolated double-shelled SiO_2/C nanotube with clear labels indicating that the C layer is the outer shell whereas the inner shell is composed of Si atom.

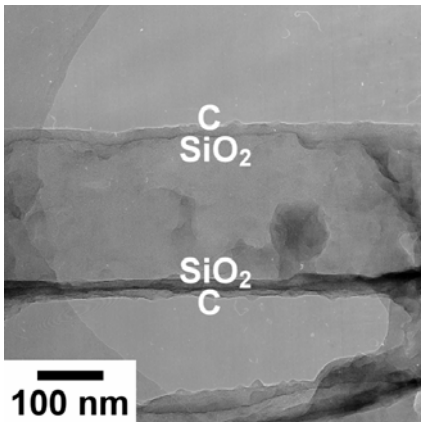

Figure 4.4 An isolated SiO_2/C nanotubes TEM image. The double-shelled nanotubes consists an outer C layer and an inner SiO_2 layer.

4.4 Conclusion

Based on the microscopy images, the diffraction, the EELS energy mapping and the spectroscopy data, we conclude that the double-shelled amorphous SiO_2/C nanotubes were prepared via the designed synthesis route. The material was fabricated via the steps shown in Scheme 4.1. First, using AAO as the substrate, Na nanotubes are grown by decomposing NaH at 623 K to form the Na@AAO reactive template. For the formation of the outer amorphous carbon shell, hexachlorobenzene (C_6Cl_6) is used as the C source to reacte with Na@AAO. Following the above Wurtz type reaction, we employed an analogous route which deposits the Si layer in the pre-grown *a*-CNT by reacting chlorosilanes with Na@*a*-C/AAO at 623 K. After the removal of AAO by HCl, we generated well-aligned coaxial double-shelled SiO_2/C nanotubes successfully. These noble fabrications of the coaxial multi-shelled nanotubes in a controlled manner may facilitate probable building of a variety of nanodevices.

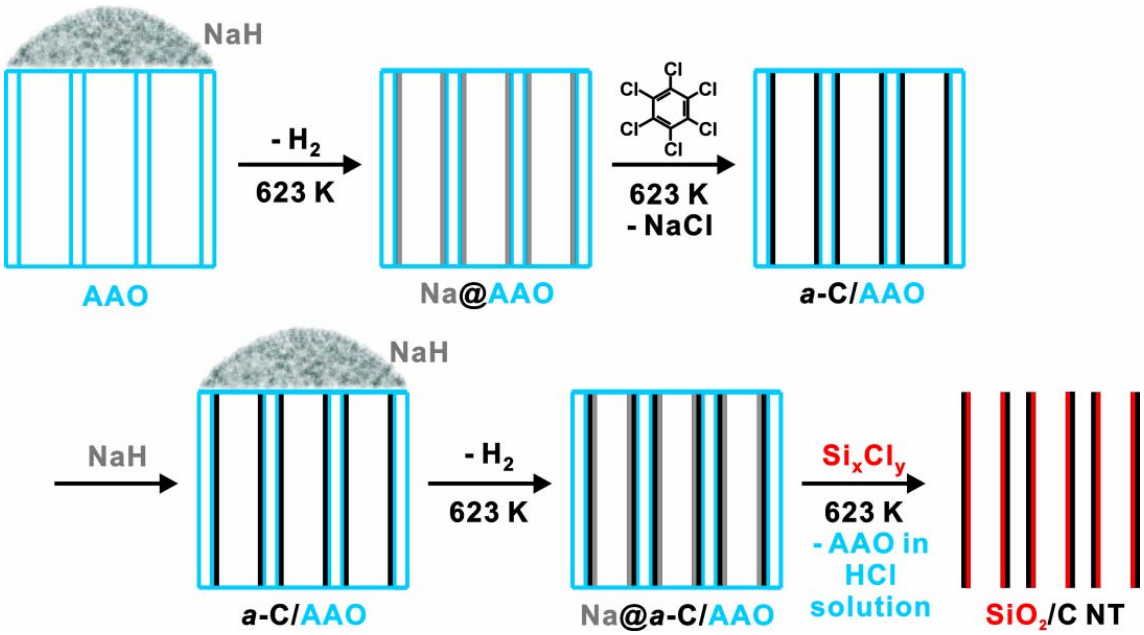

Scheme 4.1 Summary of reaction steps.

References

1. Iijima, S. *Nature* **1991**, *354*, 56.
2. Thess, A.; Lee, R.; Nikolaev, P.; Dai, H.; Petit, P.; Robert, J.; Xu, C.; Lee, Y.-H.; Kim, S.-G.; Rinzler, A. G.; Colbert, D. T.; Scuseria, G. E.; Tománek, D.; Fischer, J. E.; Smalley, R. E. *Science* **1996**, *273*, 483.
3. Collins, P. G.; Zettl, A.; Bando, H.; Thess, A.; Smalley, R. E. *Science* **1997**, *278*, 100.
4. Liu, J.; Rinzler, A. G.; Dai, H.; Hafner, J. H.; Bradley, R. K.; Boul, P. J.; Lu, A.; Iverson, T.; Shelimov, K.; Huffman, C. B.; Rodriguez-Macias, F.; Shon, Y.-S.; Lee, T. R.; Colbert, D. T.; Smalley, R. E. *Science* **1998**, *280*, 1253.
5. Kong, J.; Soh, H. T.; Cassell, A. M.; Quate, C. F.; Dai, H. *Nature* **1998**, *395*, 878.
6. Huczko, A. *Appl. Phys. A* **2000**, *70*, 365.
7. Suh, J. S.; Lee, J. S. *Appl. Phys. Lett.* **1999**, *75*, 2047.
8. Sung, S. L.; Tsai, S. H.; Tseng, C. H.; Chiang, F. K.; Liu, X. W.; Shih, H. C. *Appl. Phys. Lett.* **1999**, *74*, 197.
9. Kim, M. J.; Lee, T. Y.; Choi, J. H.; Park, J. B.; Lee, J. S.; Kim, S. K.; Yoo, J.-B.; Park, C.-Y. *Diamond Relat. Mater.* **2003**, *12*, 870.
10. Shelimov, K. B.; Moskovits, M. *Chem. Mater.* **2000**, *12*, 250.
11. Han, W.-Q.; Cumings, J.; Zettl, A. *Appl. Phys. Lett.* **2001**, *78*, 2769.
12. Chopra, N. G.; Luyken, R. J.; Cherrey, K.; Crespi, V. H.; Cohen, M. L.; Louie, S. G.; Zettl, A. *Science* **1995**, *269*, 966.
13. Suenaga, K.; Colliex, C.; Demoncy, N.; Loiseau, A.; Pascard, H.; Willaime, F. *Science* **1997**, *278*, 653.
14. Zhang, Y.; Gu, H.; Suenaga, K.; Iijima, S. *Chem. Phys. Lett.* **1997**, *279*, 264.
15. Terrones, M.; Terrones, H.; Grobert, N.; Hsu, W. K.; Zhu, Y. Q.; Hare, J. P.; Kroto, H. W.; Walton, D. R. M.; Redlich, P.; Ruhle, M.; Zhang, J. P.; Cheetham, A. K. *Appl. Phys. Lett.*

1999, *75*, 3932.

16. Han, W.; Kohler-Redlich, Ph.; Seeger, T.; Ernst, F.; Ruhle, M.; Grobert, N.; Hsu, W. K.; Chang, B. H.; Zhu, Y. Q.; Kroto, H. W.; Walton, D. R. M.; Terrones, M.; Terrones, H. *Appl. Phys. Lett.* **2000**, *77*, 1807.
17. Wang, L.-S.; Lee, C.-Y.; Chiu, H.-T. *Chem. Commum.* **2003**, 1964.
18. Weng-Sieh, Z.; Zettl, A.; Gronsky, R. *Phys. Rev. B* **1995**, *51*, 11229.
19. Robertson, J. *Mat. Sci. Eng. R* **2002**, *37*, 129.
20. Nistor, L.; Ralchenko, V.; Vlasov, I.; Khomich, A.; Khmelntkii, R.; Potapov, P.; Landuyt, J. V. *Phys. Stat. Sol. (a)* **2001**, *2*, 207.
21. Keast, V. J.; Scott, A. J.; Brydson, R.; Williams, D. B.; Bruley, J. *J. Microsc.* **2001**, *203*, 135.
22. Li, D.; Bancroft, G. M.; Kasrai, M.; Fleet, M. E.; Feng, X. H.; Tan, X. H.; Yang, B. X. *Solid State Commun.* **1993**, *87*, 613.
23. Sutherland, D. G. J.; Kasrai, M.; Bancroft, G. M.; Lui, Z. F.; Tan, K. H. *Phys. Rev. B* **1993**, *48***,** 14 989.
24. Sharp, T.; Wu, Z.; Seifert, F.; Poe, B.; Doerr, M.; Paris, E. *Phys. Chem. Minerals* **1996**, *23*, 17.
25. van Aken, P. A.; Sharp, T. G.; Seifert, F. *Phys. Chem. Minerals* **1998**, *25*, 83.